

See discussions, stats, and author profiles for this publication at: <https://www.researchgate.net/publication/260684181>

# Molecular Interactions between Thiostrepton and the TipAS Protein from *Streptomyces lividans*

ARTICLE *in* CHEMBIOCHEM · MARCH 2014

Impact Factor: 3.09 · DOI: 10.1002/cbic.201300724 · Source: PubMed

---

CITATIONS

2

---

READS

40

4 AUTHORS, INCLUDING:



Cullen L Myers

McMaster University

5 PUBLICATIONS 14 CITATIONS

SEE PROFILE



John F Honek

University of Waterloo

106 PUBLICATIONS 1,908 CITATIONS

SEE PROFILE

# Molecular Interactions between Thiostrepton and the TipAS Protein from *Streptomyces lividans*

Cullen L. Myers, Jesse Harris, Jacky C. K. Yeung, and John F. Honek<sup>\*,[a]</sup>

In *Streptomyces lividans*, the expression of several proteins is stimulated by the thiopeptide antibiotic thiostrepton. Two of these, TipAL and TipAS, autoregulate their expression after covalently binding to thiostrepton; this irreversibly sequesters the antibiotic and desensitizes the organism to its effects. In this work, additional molecular recognition interactions involved in this critical event were explored by utilizing various thiostrepton analogues and several site-directed mutants of

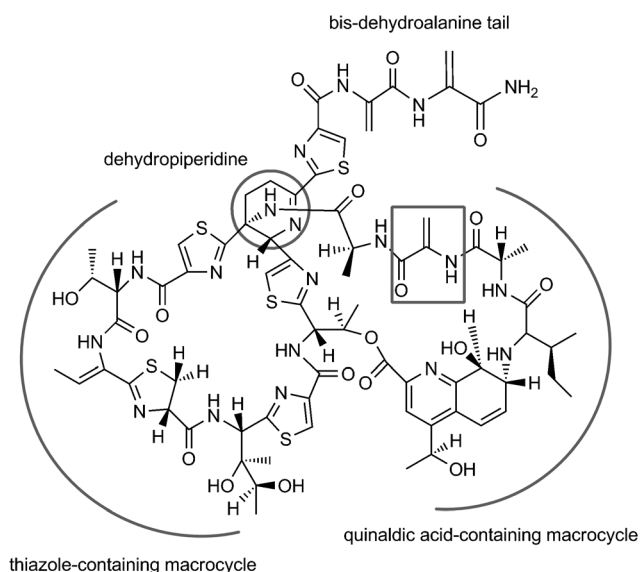
the TipAS antibiotic binding protein. Dissociation constants for several thiostrepton analogues ranged from 0.19 to 12.95  $\mu\text{M}$ , depending on the analogue. The contributions of specific structural elements of the thiostrepton molecule to this interaction have been discerned, and an unusual covalent modification between the antibiotic and a new residue in a TipAS mutant has been detected.

## Introduction

Thiostrepton (Scheme 1) is archetypal of the thiopeptides, a group of sulfur-rich, cyclic peptides that feature a diverse array of highly modified amino acids. Their structure is characterized by a macrocyclic core, from which extends a tail comprised of varying numbers of dehydroalanine (DHA) residues.<sup>[1]</sup> Thiostrepton has long been known to be a potent bactericide

of Gram-positive bacteria that results from the arrest of protein synthesis at the translocation step of the elongation cycle after binding of the antibiotic to the bacterial ribosome.<sup>[2,3]</sup> Although the antimalarial and anticancer properties of thiostrepton have also been described, the hydrophobicity of the molecule has prevented any clinical application, with the exception of its use in veterinary medicine.<sup>[4–7]</sup> Recently, biologically active thiostrepton analogues with improved aqueous solubility have been reported.<sup>[8,9]</sup>

In addition to the aforementioned biological properties, thiostrepton is known to regulate gene expression in certain *Actinomycetes*. This was first discovered in *Streptomyces lividans*, where elevated levels in the expression of several proteins were noted in the presence of the antibiotic.<sup>[10]</sup> The most abundant of these, referred to as TipAL and TipAS, are the in-frame products expressed from independent transcription start sites on the *tipA* gene. This gene is autoregulated by TipAL, which features a DNA binding N-terminal domain characteristic of the MerR/Sox family of transcriptional regulators. The N-terminal domain of TipAL binds to the *tipA* promoter, and its affinity for this promoter is greatly enhanced by the irreversible binding of thiostrepton to the C-terminal domain of the protein.<sup>[10,11]</sup> The C-terminal domain of TipAL is independently expressed as TipAS after initiation of transcription from the internal transcription start site in the *tipA* gene. Enhanced binding of TipAL to the *tipA* promoter consequently promotes the recruitment of RNA polymerase, which leads to gene expression that is skewed towards greater production of TipAS.<sup>[11–14]</sup> As this protein represents the thiostrepton-binding domain, the bacteria become resistant to the effects of the antibiotic as it becomes sequestered. The predominant form of natural thiostrepton resistance occurs among producers of the antibiotic (*Streptomyces cyaneus* and *Streptomyces laurentii*), which express a 23S rRNA methyltransferase that catalyzes AdoMet-dependent methylation of a key adenine residue at the target



**Scheme 1.** Structure of thiostrepton ( $M_w = 1664.50$  Da).

[a] Dr. C. L. Myers, J. Harris, J. C. K. Yeung, Prof. J. F. Honek  
Department of Chemistry, University of Waterloo  
200 University Avenue West, Waterloo, Ontario N2L 3G1 (Canada)  
E-mail: jhonek@uwaterloo.ca

Supporting information for this article is available on the WWW under <http://dx.doi.org/10.1002/cbic.201300724>.

site of thiostrepton, thereby preventing drug binding to the ribosome.<sup>[15,16]</sup> Interestingly, *S. lividans* and other *Actinomycetes* found to possess and express the *tipA* gene do not themselves produce thiostrepton, any other thiopeptides, or corresponding resistance enzymes.<sup>[17]</sup>

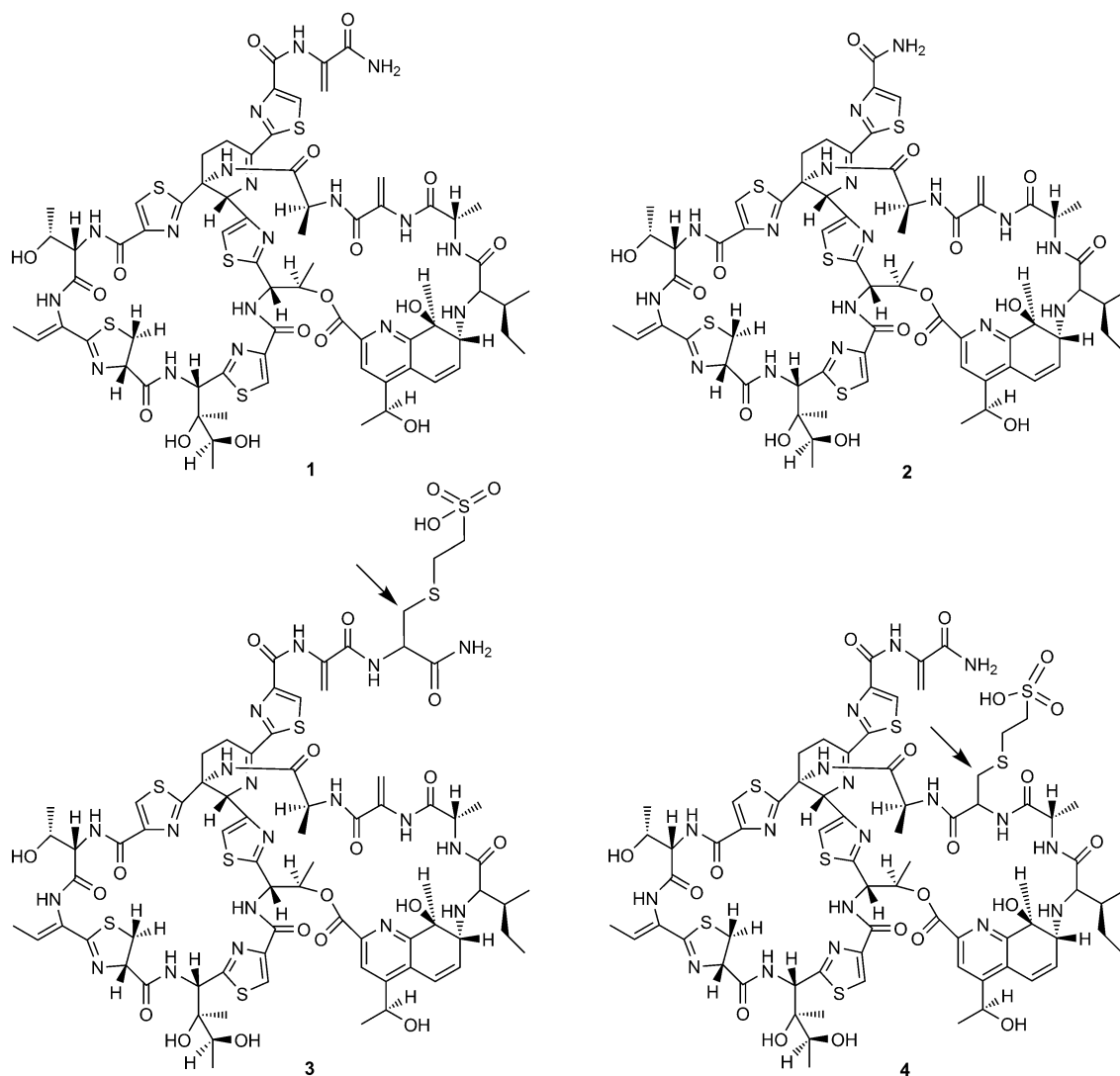
The irreversible binding of TipAL or TipAS to thiostrepton results from a covalent bond formed between Cys214 of the protein and a dehydroalanine (DHA) residue from the tail of the antibiotic, but evidence suggestive of a stable, reversible interaction between thiostrepton and TipAL or TipAS has also been noted. Early studies involved the use of a thiostrepton-based affinity column for the isolation of thiostrepton-binding proteins from cell lysates.<sup>[11,18]</sup> As thiostrepton was immobilized onto a solid support through its DHA tail, protein capture by this column occurred solely through noncovalent interactions. Moreover, several thiopeptides possessing DHA tails were shown to covalently bind TipAL/TipAS in the same manner as thiostrepton, but a subset of tailless analogues of these compounds, including thiostrepton, were able to accomplish *ptipA*

induction in vivo despite an inability to covalently bind to TipAL/TipAS.<sup>[19]</sup> Nevertheless, knowledge of the detailed molecular nature of these important noncovalent interactions remains limited. In order to more fully explore these interactions, various thiostrepton analogues (Scheme 2) and site-directed mutants of the TipAS antibiotic binding protein were utilized to directly examine the antibiotic–TipAS interaction. Additionally, a new covalent interaction between the antibiotic and TipAS was identified by investigation of Cys214Ser and Cys214Ala site-directed mutants of the protein.

## Results and Discussion

### The importance of noncovalent TipAS–thiostrepton interactions

In the absence of a molecular structure for the thiostrepton–TipAS complex, computational docking experiments were performed to obtain an overview of the protein–antibiotic interac-



**Scheme 2.** Thiostrepton analogues used in this study.

tion. The results of these simulations were consistent with the NMR studies of Kahmann et al., to the extent that several of the lowest energy poses showed the thiostrepton core embedded in the hydrophobic interior of TipAS, with the DHA tail within bonding proximity of the Cys214 protein residue (Figures 1 and 2).<sup>[14]</sup> However, in general, much variation was seen

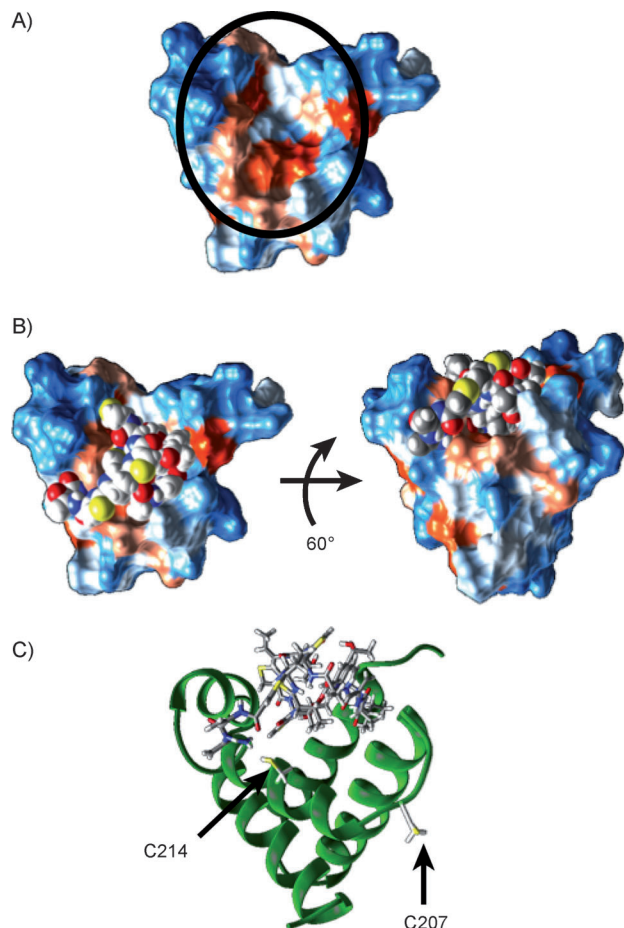


**Figure 1.** Modeling the TipAS–thiostrepton interaction. Molecular graphics were generated by using the UCSF Chimera Package version 1.7. A) TipAS (PDB ID: 1NY9) is shown as a space-filling model and mapped on the basis of hydrophobicity; red/orange denotes greater hydrophobicity. The hydrophobic cleft forming the proposed thiostrepton binding site is circled. B) Docking of thiostrepton (PDB ID: 1E9W) into the proposed binding site on TipAS with Molegro Virtual Docker. One of several poses from virtual docking experiments is depicted in which the DHA tail from thiostrepton is positioned within bonding distance of the Cys214 thiol from TipAS. C) Positions of cysteine residues in TipAS (green ribbons) docked with thiostrepton.

in the position of the thiostrepton tail among all poses, which could be attributed to inherent flexibility of this region of the thiostrepton molecule.<sup>[20]</sup> On the other hand, little deviation of the position of the thiostrepton core was evident across the entire set of results.

Initially, a truncated version of TipAS (TipASt), representing the region of the protein that associates with thiostrepton, was recombinantly generated for use in examinations of the protein–antibiotic interaction. However, mass spectrometric

analysis of the products from the reaction between TipASt and thiostrepton found that, in contrast to full-length TipAS, which reacted completely to form a single adduct with thiostrepton (Figure 3A; Figure S1 in the Supporting Information), the majority of TipASt remained unreacted, and adducts with one or two thiostrepton molecules were detected (Figure 3B). This was attributed to structural differences between TipAS and TipASt, which was verified by circular dichroism measurements (Figure S2). Subsequent investigations were thus carried out only on the full-length protein or its point mutants, as these structural differences in TipASt likely result in the elimination of the binding region that forms noncovalent associations with thiostrepton, as depicted in Figure 2. Indeed, the significance of these noncovalent associations was highlighted in qualitative examinations of the protein–antibiotic interaction by using fluorescence spectroscopy, which showed a reduction in the intrinsic fluorescence of TipAS after interaction with analogue 2, which forms no covalent adduct with thiostrepton (Figure S3).

#### The absence of the reactive amino acid on TipAS does not preclude covalent binding

Covalent binding between TipAS and thiostrepton most likely proceeds through a Michael addition between the cysteine thiol and the terminal DHA on the thiostrepton tail.<sup>[18,19]</sup> With a view towards *in vitro* examinations of the noncovalent associations, it was thought that covalent bond formation would be prevented in a TipAS mutant where the reactive cysteine (Cys214) was replaced by a residue presenting a less favorable Michael donor as compared to that provided by the thiol group of cysteine. This was first attempted by substituting a serine residue at this site, but unexpectedly, thiostrepton was determined to be covalently bound to this mutant to a similar extent as the native protein under the same conditions (Figure 3C). An alanine mutant was therefore prepared, as it was thought that the hydroxy on the serine side chain might have acted as an alternate nucleophile, but again, covalent addition to the protein was detected (Figure 3D). Thiostrepton addition to an alternate amino acid residue appeared apparent in these point mutants, and the second cysteine in the protein, Cys207, seemed the most probable candidate, though nothing is known concerning reactivity at this residue.

The identification of the reactive residue was sought through mass spectrometric analyses of the peptide fragments resulting from CNBr digestion of these protein–thiostrepton complexes. Such digestion gives the location of these cysteines on distinct peptide fragments (Figure S4), and Figure 4 shows the HPLC chromatograms from separation of the CNBr digestion products of unbound and thiostrepton-bound mutants. The experimentally determined masses for all peptide fragments generated from the cleavage of unbound TipAS were in agreement with their predicted values, with the exception of peptide D, for which a higher mass than expected was observed due to the oxidation of cysteine to cysteic acid by CNBr (Table S3).<sup>[21–23]</sup> It is evident that the digests from thiostrepton-bound proteins are lacking in product D but, at the same time,

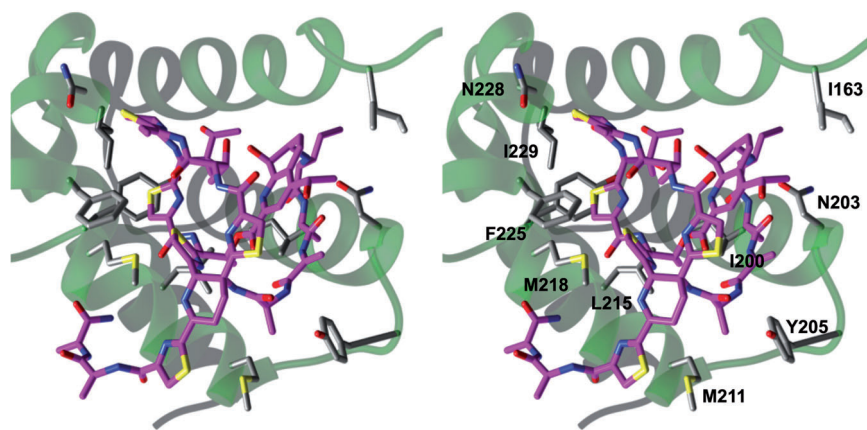


**Figure 2.** Noncovalent interactions in the thioestrepton binding site. This stereoimage depicts the top-down view of the simulated docking of thioestrepton on to TipAS. Amino acid residues potentially engaging in noncovalent interactions with thioestrepton are shown. Most evident are possible hydrophobic interactions between the quinaldic acid-containing macrocycle and Ile163, Ile200, and Tyr205, and between the thiazole-containing macrocycle and Leu215, Tyr219, Phe225, and Ile229, with possible  $\pi$ -stacking that sandwiches a thiazole between Tyr219 and Phe225. In addition, polar interactions or hydrogen bonding might occur between Asn203 and the peptide backbone of the quinaldic acid-containing macrocycle, Asn228 with a thiazole from the thiazole-containing macrocycle, and Met211 and Met218 with the DHA tail.

the addition site. Under the cleavage conditions utilized here, this lone cysteine in the unbound mutant proteins was present entirely as cysteic acid after CNBr treatment. Therefore, peptide D1, which appears in the digests of thioestrepton complexes with TipAS point mutants, results from the addition of thioestrepton to peptide D when the oxidation of Cys207 has not occurred. Given that CNBr treatment was performed after the formation of thioestrepton complexes with these point mutants, it was clear that the reaction of the protein with thioestrepton rendered the cysteine thiol unavailable for reaction with CNBr, confirming addition of thioestrepton to Cys207 in these point mu-

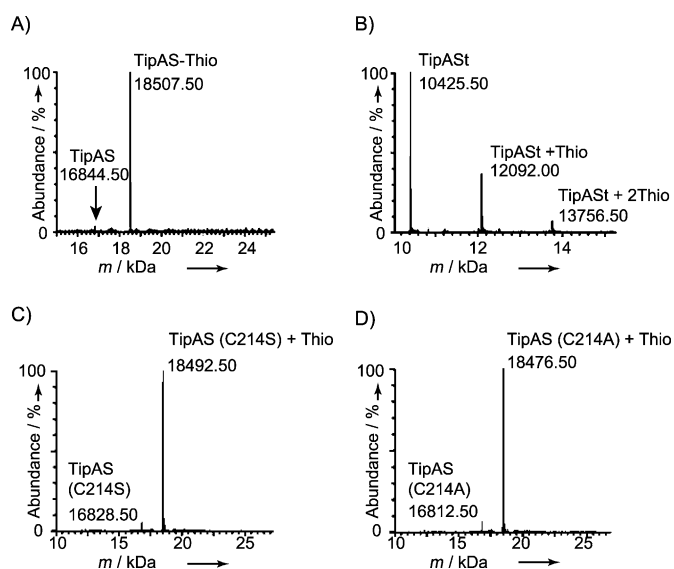


**Figure 3.** Reaction of thioestrepton with TipAS or its variants. Deconvoluted ESI mass spectra of the products from the thioestrepton reaction with A) TipAS; 18 507.5 corresponds to the addition of a single thioestrepton molecule; B) truncated TipAS; 12 092.00 corresponds to the addition of one thioestrepton molecule to TipAS, and 13 756.50 corresponds to the addition of two thioestrepton molecules to TipAS; C) the Cys214Ser point mutant of TipAS; and D) the Cys214Ala point mutant of TipAS. Masses of the unbound point mutants are 16 828.5 and 16 812.5, whereas thioestrepton-bound proteins have masses of 18 492.50 and 18 476.50.

feature a product(s) emerging after 39–44 min. The mass of this product, designated D1, is consistent with the addition of thioestrepton (with a mass of 1680 Da after CNBr treatment; Supporting Information) to peptide D (Table S3). The fortuitous oxidation of cysteine to cysteic acid during CNBr cleavage enabled confirmation of Cys207, which is within this peptide, as

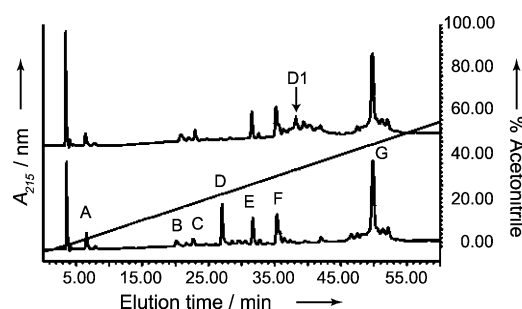


**Figure 4.** HPLC of CNBr digests from TipAS (or its point mutants) before and after the reaction with thioestrepton. The lower trace shows the chromatogram resulting from HPLC separation of TipAS or its variants after CNBr digestion; the upper trace shows the CNBr digestion products from protein-thioestrepton complexes. ESI-MS analysis of the HPLC products is summarized in the Supporting Information (Table S3). The product designated D1 appeared only in the digests of protein-thioestrepton complexes, and the mass determined for this product was consistent with peptide D bound to thioestrepton (mass: 4082 Da). The peak eluting immediately after D1 contained formylated D1.

tants. Though observed here in an artificial system, these results nonetheless provide formative understanding of the protein-antibiotic interaction by demonstrating that the noncovalent association is of sufficient affinity to immobilize the core of the antibiotic on the protein and allow for reorientation of the Michael acceptor on the flexible thioestrepton tail to a position amenable for addition with the less favored Cys207.

### The thioestrepton tail is important for noncovalent binding

The thioestrepton analogues depicted in Scheme 2 were facilitative for isothermal titration calorimetry (ITC) studies that were employed for quantification of the noncovalent binding affini-



ty, as well as for the differentiation of specific contributions from regions of the thiostrepton molecule to TipAS binding. Thiostrepton analogue **3** (Scheme 2) was prepared, in which the reactive DHA was blocked with 2-mercaptoethanesulfonate (MENZA) and, under the same conditions, analogue **4** (Scheme 2) was generated from the truncated thiostrepton derivative **1**. For this molecule, MENZA was appended to the DHA residing on the central core of the thiostrepton molecule. Tail-modified derivatives of **1** have been prepared elsewhere; however, the previous syntheses were performed in buffered conditions at a pH lower than that utilized in this study, which directed addition to the tail DHA.<sup>[24]</sup> Neither derivative **3** nor **4** covalently bound TipAS within the time span of the ITC experiment (confirmed by ESI mass spectrometry analyses), and all analogues displayed improved aqueous solubility relative to thiostrepton.

Analogues **2**, **3**, and **4** bound TipAS with dissociation constants of  $(5.38 \pm 0.03) \mu\text{M}$ ,  $(0.19 \pm 0.01) \mu\text{M}$ , and  $(12.95 \pm 0.01) \mu\text{M}$ , respectively, whereas **1** bound with a dissociation constant of  $(0.21 \pm 0.002) \mu\text{M}$  to the Cys214Ala mutant (Figure 5). In each case, the binding isotherm exhibited 1:1 binding stoichiometry and, in general, the measured dissociation constants portrayed a high affinity interaction, in line with the qualitative observations presented earlier. It has been also suggested that the ability of thiopeptides to covalently bind

TipAS correlates positively with the number of DHAs in the tail region.<sup>[19]</sup> Comparative evaluations of the noncovalent binding of analogues with different tail structures, performed here, found the dissociation constant for **2** to be approximately 30 times greater than that for **1** or **3**, signifying that the presence of a tail region is also important in noncovalent binding. This contribution is secondary to the association between the macrocyclic thiostrepton core and the amino acid residues that construct the antibiotic binding site, which was particularly highlighted by the diminished noncovalent binding affinity of TipAS for **4**. The presence of the MENZA moiety on the macrocyclic core of thiostrepton in this analogue (Scheme 2) undoubtedly interfered with noncovalent protein–antibiotic associations that would include the hydrophobic, polar, and hydrogen bonding interactions implied from the docking simulations (Figure 2). Additionally, despite possessing a tail region, covalent adducts between analogue **4** and TipAS were not detected during the course of the ITC experiments (such complexes occurred to a minor extent only after extended incubation times), which emphasizes the importance of the specific noncovalent interaction for irreversible binding of the antibiotic to occur. Noncovalent immobilization of the macrocyclic thiostrepton core also accounts for the formation of a covalent complex with analogue **1**. The lone DHA in the tail of **1** contains a reactive olefin, and this Michael acceptor would not initially be in an orientation suitable for addition, due to the shortened tail length of this analogue. However, when noncovalently bound to TipAS, the rotational flexibility of the DHA tail of **1** can reorient the position of this DHA, which subsequently facilitates Michael addition. Irreversible addition of this analogue would be expected to occur to a lesser degree than for unmodified thiostrepton, as was reflected in mass spectrometric analysis of the reaction between TipAS and **1** (Figure S5).

## Conclusions

This work has dissected several of the contributions of the macrocyclic core and tail region of thiostrepton to its noncovalent interaction with TipAS. A previously unassigned involvement of the tail region in this interaction has been reported, and the role of the noncovalent interaction in directing the irreversible protein–antibiotic binding has been clarified. These findings are very likely to be broadly applicable to thiopeptide–protein interactions and consequent thiopeptide-induced activities that occur in numerous *Actinomycetes*. Recent studies have called attention to the biological relevance of TipAS (and TipAL), and it seems plausible that these proteins mediate thiopeptide-specific insensitivity in organisms that do not manufacture these compounds.<sup>[25,26]</sup> Hence, our findings could have broader implications in the design of thiopeptide-based antimicrobial compounds that evade noncognate resistance mechanisms and could be of further relevance for heterologous production of such compounds. Furthermore, the findings reported here provide a basis for further understanding these critically important molecular recognition events in the additional biological activities of thiostrepton.

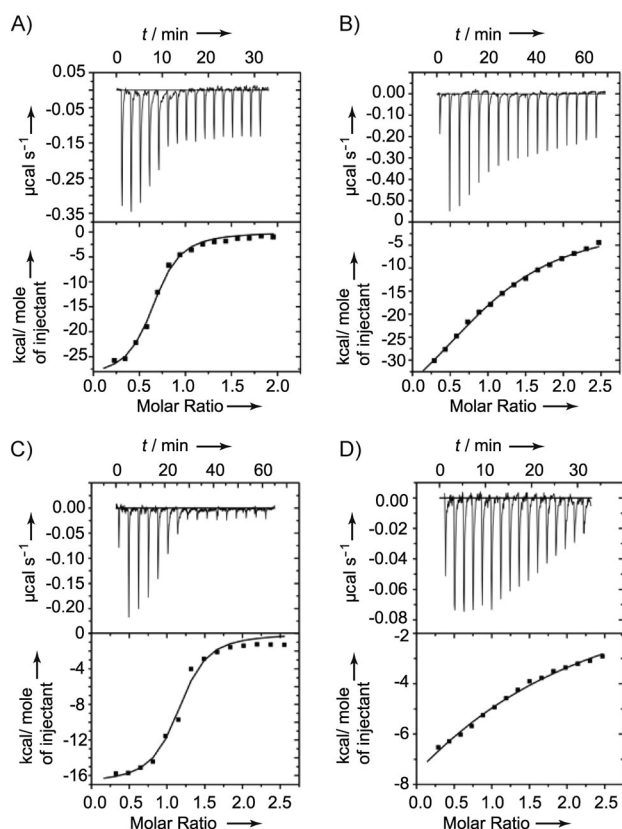


**Figure 5.** Evaluation of noncovalent TipAS–thiostrepton binding by isothermal titration calorimetry. Upper panels show the titration curves, and lower panels show these data fitted to the isotherm, with 1:1 binding stoichiometry for titrations between the Cys214Ala mutant of TipAS with A) **1** and TipAS with B) **2**, C) **3**, and D) **4**.

## Experimental Section

**Chemicals and reagents:** Dimethyl sulfoxide, dimethyl formamide, and trifluoroacetic acid were purchased from Caledon Laboratory Chemicals (Georgetown, Ontario, Canada), and triethylamine was obtained from EMD Millipore (Billerica, MA, USA). Thiostrepton, sodium 2-mercaptoethanesulfonate (MENSA), sodium cyanoborohydride, cyanogen bromide, and diethylamine were purchased from Sigma (Oakville, Ontario, Canada).

**Plasmid construction and protein expression:** The DNA sequence encoding TipAS and a sequence encoding the 90 C-terminal amino acids of TipAS were amplified from *S. lividans* genomic DNA by PCR. Proteins were produced in an *Escherichia coli* expression system (pET28a expression vector, *E. coli* BL21 cells) and purified by nickel affinity chromatography. Point mutations (Cys214Ala and Cys214Ser) were introduced into TipAS by PCR-driven overlap and extension, and the mutants were purified under the same conditions as the native protein. Additional details of these methods are provided in the Supporting Information.

**Protein–antibiotic reactions:** TipAS or its variants were reacted with thiostrepton according to the method described by Chiu et al.<sup>[18]</sup> Briefly, after reduction with 3.5 molar equivalents of sodium cyanoborohydride, proteins were incubated with a fivefold molar excess of thiostrepton (added as a solution in DMSO) at room temperature for 60 min. The reaction mixture was passed through a 0.2 µm cellulose acetate filter to remove precipitated antibiotic and then washed in a NanoSep centrifugal device (Pall Life Sciences, Mississauga, Ontario, Canada) to remove excess DMSO and unreacted antibiotic.

**Isothermal titration calorimetry:** Isothermal titration calorimetry (ITC) experiments were performed utilizing an ITC<sub>200</sub> microcalorimeter (GE Healthcare, Baie d'Urfe Quebec, Canada). Protein utilized in the experiments was dialyzed extensively at 4°C against a buffer comprised of Tris (20 mM, pH 7.5), glycerol (10%, v/v), and 2-mercaptoethanol (5 mM). The dialysate was used to prepare working solutions of thiostrepton analogues (100 µM), with 15% DMSO (v/v). Titrations consisted of 16 or 17 injections (2.0–2.2 µL) of antibiotic solution into a sample cell containing protein (7 µM), with DMSO at 15% (v/v). The heat of dilution was obtained from injections of the respective antibiotic solutions into buffer containing no protein (with DMSO at 15% (v/v)). After subtraction of the heats of dilution, titration curves were generated and analyzed by using Origin 7.0 software (Microcal), and the data were fitted by using a model for one set of binding sites.

**Cyanogen bromide digestion:** Unbound protein or protein–thiostrepton complex (ca. 1–2 mg) was precipitated from CH<sub>3</sub>CO<sub>2</sub>H. The dried precipitate was dissolved in degassed 87.5% formic acid (800 µL). Cyanogen bromide, prepared as a solution (1 M) in CH<sub>3</sub>CN (degassed), was added to each sample at a 200 molar excess of methionine residues, and the mixture was incubated in the dark at room temperature for 24 h. The reaction was quenched by the addition of 5 volumes of doubly distilled water and then lyophilized.

**HPLC separation and mass spectrometry of cyanogen bromide cleavage products:** The lyophilized products from cyanogen bromide cleavage were dissolved in 0.1% TFA and fractionated by reversed-phase HPLC on a Waters µBondapak C18 column (10 µm, 3.9×300 mm), using a Waters 600S gradient controller. The polar and nonpolar elution solvents were 0.1% TFA and CH<sub>3</sub>CN (containing 0.1% TFA), respectively. The cleavage products were eluted over a linear, increasing gradient of the nonpolar solvent (0–100% over 100 min), monitoring at 215 nm, at a flow rate of

0.8 mL min<sup>−1</sup>. The collected fractions were diluted in H<sub>2</sub>O/CH<sub>3</sub>CN (1:1, containing 0.2% formic acid) and then introduced into a Micromass Q-TOF Ultima Global mass spectrometer (Waters) in positive ion mode. The spectra were analyzed by using MaxEnt software (Waters).

**Preparation of thiostrepton analogues:** Truncated thiostrepton derivatives **1** and **2** were prepared according to a published method, and **3** and **4** were prepared as previously described.<sup>[8,9]</sup> Synthetic details are provided in the Supporting Information.

**Molecular modeling:** Protein Data Bank (PDB) files for TipAS (PDB ID: 1NY9) and thiostrepton (PDB ID: 1E9W) were individually imported into Molegro Virtual Docker 5.0 (Molegro ApS, Aarhus, Denmark).<sup>[27]</sup> TIPAS was designated as the protein/receptor and thiostrepton as the ligand. Both structures were edited to include bonds missing from the PDB file, correct improper bonds, add explicit hydrogen atoms, and assign missing charges. Also, the flexible bonds in thiostrepton were allowed their full range of rotation. The thiostrepton binding site (cavity) was defined as a region that encompassed but was not entirely restricted to the binding site proposed by Kahmann et al.<sup>[14]</sup> The entire docking simulation consisted of 15 runs of 1500 iterations each, with the MolDock SE heuristic search algorithm and the MolDock scoring function.<sup>[27]</sup> Poses exhibiting the 20 lowest energies were retained for further inspection.

## Acknowledgements

We thank Dr. Thorsten Dieckmann for access to calorimetry facilities, Dr. Richard Smith of the WATSPEC Mass Spectrometry Facility at the University of Waterloo for technical advice and assistance, and Dr. Gerard Wright for providing *Streptomyces lividans* 2K4 genomic DNA. Financial support was generously provided by the Natural Sciences and Engineering Research Council of Canada (NSERC), the Ontario Government, and the University of Waterloo.

**Keywords:** antibiotic resistance • bioorganic chemistry • isothermal titration calorimetry • thiostrepton • TipAS

- [1] M. C. Bagley, J. W. Dale, E. A. Merritt, X. Xiong, *Chem. Rev.* **2005**, *105*, 685–714.
- [2] G. Rosendahl, S. Douthwaite, *Nucleic Acids Res.* **1994**, *22*, 357–363.
- [3] G. Lentzen, R. Klinck, N. Matassova, F. Aboul-ela, A. I. H. Murchie, *Chem. Biol.* **2003**, *10*, 769–778.
- [4] B. Clough, M. Strath, P. Preiser, P. Denny, I. Wilson, *FEBS Lett.* **1997**, *406*, 123–125.
- [5] S. Schoof, G. Pradel, M. N. Aminake, B. Ellinger, S. Baumann, M. Potowski, Y. Najajreh, M. Kirschner, H.-D. Arndt, *Angew. Chem. Int. Ed.* **2010**, *49*, 3317–3321; *Angew. Chem.* **2010**, *122*, 3389–3393.
- [6] J. M.-M. Kwok, S. S. Myatt, C. M. Marson, R. C. Coombes, D. Constantini-dou, E. W.-F. Lam, *Mol. Cancer Ther.* **2008**, *7*, 2022–2032.
- [7] N. S. Hegde, D. A. Sanders, R. Rodriguez, S. Balasubramanian, *Nat. Chem.* **2011**, *3*, 725–731.
- [8] S. Schoof, S. Baumann, B. Ellinger, H.-D. Arndt, *ChemBioChem* **2009**, *10*, 242–245.
- [9] C. L. Myers, P. C. Hang, G. Ng, J. Yuen, J. F. Honek, *Bioorg. Med. Chem.* **2010**, *18*, 4231–4237.
- [10] T. Murakami, T. G. Holt, C. J. Thompson, *J. Bacteriol.* **1989**, *171*, 1459–1466.
- [11] D. J. Holmes, J. L. Caso, C. J. Thompson, *EMBO J.* **1993**, *12*, 3183–3191.
- [12] M. L. Chiu, P. H. Viollier, T. Katoh, J. J. Ramsden, C. J. Thompson, *Biochemistry* **2001**, *40*, 12950–12958.

- [13] N. Ali, P. R. Herron, M. C. Evans, P. J. Dyson, *Microbiology* **2002**, *148*, 381–390.
- [14] J. D. Kahmann, H.-J. Sass, M. G. Allan, H. Seto, C. J. Thompson, S. Grzesiek, *EMBO J.* **2003**, *22*, 1824–1834.
- [15] A. Bechthold, H. G. Floss, *Eur. J. Biochem.* **1994**, *224*, 431–437.
- [16] M. S. Dunstan, P. C. Hang, N. V. Zelinskaya, J. F. Honek, G. L. Conn, *J. Biol. Chem.* **2009**, *284*, 17013–17020.
- [17] C. Vasant Kumar, *FEMS Microbiol. Lett.* **1994**, *118*, 107–111.
- [18] M. L. Chiu, M. Folcher, P. Griffin, T. Holt, T. Klatt, C. J. Thompson, *Biochemistry* **1996**, *35*, 2332–2341.
- [19] M. L. Chiu, M. Folcher, T. Katoh, A. M. Puglia, J. Vohradsky, B. S. Yun, H. Seto, C. J. Thompson, *J. Biol. Chem.* **1999**, *274*, 20578–20586.
- [20] P. C. Hang, J. F. Honek, *Bioorg. Med. Chem. Lett.* **2005**, *15*, 1471–1474.
- [21] E. Gross, *Methods Enzymol.* **1967**, *11*, 238–255.
- [22] R. D. Hsiang, M. W. Cole, *Methods Cell Biol.* **1978**, *18*, 189–228.
- [23] K. Klarskov, F. Verte, G. Van Driessche, T. E. Meyer, M. A. Cusanovich, J. Van Beeumen, *Biochemistry* **1998**, *37*, 10555–10562.
- [24] M. N. Aminake, S. Schoof, L. Sologub, M. Leubner, M. Kirschner, H.-D. Arndt, G. Pradel, *Antimicrob. Agents Chemother.* **2011**, *55*, 1338–1348.
- [25] A. Giardina, R. Alduina, E. Gottardi, V. Di Caro, R. D. Süssmuth, A. M. Puglia, *Microb. Cell Fact.* **2010**, *9*, 44.
- [26] C. Li, F. Zhang, W. L. Kelly, *Mol. Biosyst.* **2011**, *7*, 82–90.
- [27] R. Thomsen, M. H. Christensen, *J. Med. Chem.* **2006**, *49*, 3315–3321.

---

Received: November 18, 2013

Published online on February 24, 2014